Earth and Planetary Science Letters 345-348 (2012) 9–17

Contents lists available at SciVerse ScienceDirect

Earth and Planetary Science Letters

journal homepage: www.elsevier.com/locate/epsl

Letters

Boron incorporation into calcite during growth: Implications for the use of boron in carbonates as a pH proxy

E. Ruiz-Agudo [a,b,*], C.V. Putnis [b], M. Kowacz [c], M. Ortega-Huertas [a], A. Putnis [b]

[a] Department of Mineralogy and Petrology, University of Granada, Fuentenueva s/n, 18071 Granada, Spain
[b] Institut für Mineralogie, Universität Münster, Corrensstrasse 24, 48149 Münster, Germany
[c] Instituto de Tecnologia Química e Biológica, Universidade Nova de Lisboa, Av. da República, 2780-157 Oeiras, Portugal

ARTICLE INFO

Article history:
Received 13 January 2012
Received in revised form
29 May 2012
Accepted 4 June 2012
Editor: G. Henderson
Available online 20 July 2012

Keywords:
calcite growth
boron incorporation
pH-proxy
AFM

ABSTRACT

Current interest in boron incorporation into carbonates arises from the observation that the isotopic composition of carbonates depends on the pH of the fluid from which they precipitated. This finding opened the possibility of using boron isotopic composition of natural carbonates as a paleo-pH proxy. In this study, coprecipitation of boron by calcite was investigated using Atomic Force Microscopy (AFM), as a function of pH, supersaturation and boron concentration. In situ AFM observations reported here provide experimental evidence of boron incorporation into calcite, which takes place to a greater extent at high pH (9.5) and under close to equilibrium conditions. Moreover, we report nanoscale observations that give indirect evidence of the incorporation of boron in non-lattice sites. Step-specific interactions of tetrahedrally-coordinated boron with calcite obtuse steps during growth are revealed as a reduction in the obtuse-step spreading rate as well as rounding and roughening of such steps. Our results suggest that, together with changes in pH, variations in the calcification rate or the calcite crystallographic form in which boron is incorporated are important factors to consider when using boron in carbonates as a pH proxy, as these factors could also influence the amount of boron incorporated during growth and possibly the boron isotopic signature.

1. Introduction

Direct measurements of average ocean surface water pH show acidification of oceans since preindustrial times, possibly as a consequence of the increase in the atmospheric pCO_2, primarily related to fossil fuel combustion (Royal Society, 2005). However, long-term variations of oceanic pH are not well documented and only information extracted from indirect proxies is available (Rollion-Bard and Erez, 2010). Knowledge of paleo-pH is essential in order to constrain past changes in the atmospheric CO_2 concentration and to obtain insights into the evolution of Earth's climate. Reconstructions of ancient ocean pH are currently based on a theoretical model of the boron isotopic composition ($\delta^{11}B$) of marine biocarbonates. This model relies on a large predicted isotopic fractionation between the two primary aqueous boron species in seawater (boric acid, $B(OH)_3$ and borate ion, $B(OH)_4^-$) at normal concentrations of boron in natural waters and on the pH dependence of their relative abundance (e.g. Sanyal et al., 1995). The distribution of these two dominant aqueous species is related to pH according to the reaction

$$B(OH)_3 + H_2O \Leftrightarrow B(OH)_4^- + H^+$$

with an equilibrium constant $K = 10^{-8.597}$ at 25 °C and salinity = 35 (Dickson, 1990). $B(OH)_3$ is significantly enriched in ^{11}B relative to $B(OH)_4^-$ with an isotope equilibrium constant at 25 °C ($^{11-10}K_B$) for seawater (salinity = 35, total boron = 0.01 mol kg^{-1} H_2O) of 1.0272 ± 0.0006 (Klochko et al., 2006). In this model it is generally assumed that tetrahedrally-coordinated boron, $B(OH)_4^-$, is solely or predominantly the aqueous species incorporated into calcite, as suggested by the similarities between the boron isotopic composition of B-bearing carbonates and aqueous $B(OH)_4^-$ (Hemming and Hanson, 1992). If this were the case, boron concentration in carbonates would increase with increasing pH, given the correspondence between $B(OH)_4^-$ and pH. Positive trends between B concentrations and $\delta^{11}B$ and the pH of the precipitating fluid have been observed in inorganic experiments (Hobbs and Reardon, 1999; Sanyal et al., 2000) indicating that indeed $\delta^{11}B$ and, possibly, the boron composition of carbonates, reflect changes in the pH of the solution from which they precipitated. This technique has mainly been used in corals and foraminifera (e.g. Vengosh et al., 1991; Spivack et al., 1993;

* Corresponding author at: Department of Mineralogy and Petrology, University of Granada, Fuentenueva s/n, 18071 Granada, Spain.
E-mail address: encaruiz@ugr.es (E. Ruiz-Agudo).

0012-821X/$ - see front matter © 2012 Published by Elsevier B.V.
http://dx.doi.org/10.1016/j.epsl.2012.06.032

Gaillardet and Allègre, 1995; Sanyal et al., 1997; Rollion-Bard and Erez, 2010; Rollion-Bard et al., 2011; Trotter et al., 2011).

Although the use of boron isotopes has been proven to be an undoubtedly powerful tool for the reconstruction of past seawater pH, there are still several aspects that require more investigation and would be essential to know in order to fully constrain the use of this proxy. First, it seems obvious that an exact knowledge of isotopic and equilibrium constants would be necessary in order to precisely constrain the variation of the boron isotopic composition of borate with pH, as they will influence sensitivity of the δ^{11}B-pH curve (Pagani et al., 2005; Hönisch et al., 2007; Pagani and Spivack, 2007). In this sense, Klochko et al. (2006) have experimentally determined a value for $^{11-10}K_B$ of seawater (1.0272) significantly larger than the value used in numerous paleo-pH studies (which is very similar to that theoretically determined by Kakihana et al. (1977), 1.0194). This results in a different $\delta^{11}B_{borate}$-pH curve, which is used as a reference for boron isotopic composition of the carbonate minerals that serve as a proxy for seawater isotopic compositions. An additional concern arises from the fact that some marine carbonates calcify from an internal fluid with a composition and pH different from that of the surrounding seawater, and most of the time the exact pH at the site of calcification and its evolution during the calcification process is unknown. This has been shown, for example, for some foraminifera species, such as *G. sacculifer*, which raises its pH to 8.6 in daylight relative to that of ambient seawater (pH=8.2) (e.g. Jorgensen et al., 1985), or for corals such as *Galaxea*, which increases pH from 8.2 to 9.3 in the calcifying fluid (e.g. Al-Horani et al., 2003). As well, the value of $\delta^{11}B_{carbonate}$ would differ from the theoretical $\delta^{11}B_{borate}$ if trigonal boron, $B(OH)_3$, were also incorporated into the carbonate due to changes in pH and/or other physical conditions, such as growth rate, as some studies have suggested (Pagani et al., 2005; Klochko et al., 2009; Rollion-Bard et al., 2011). This would, therefore make the use of B isotopes questionable as a reliable paleo-pH proxy.

These considerations aside, there are other questions related to the way in which boron is incorporated into carbonates that remain unresolved and that this study explores. Although the increase in incorporated boron with increasing pH can be explained largely by the change in speciation, the possibility cannot be ruled out that other factors, including kinetic effects associated with changes in growth rate (Hobbs and Reardon, 1999), may have an influence. Furthermore, previous studies have shown that boron coprecipitation by calcite is controlled by the structure of the growing surfaces (Hemming et al., 1998). Face/site-specific interactions of boron with calcite surfaces could also affect the extent of boron incorporation (Hobbs and Reardon, 1999). Therefore, a robust mechanistic knowledge of the incorporation of boron species into carbonates during growth remains critical for constraining the use of the boron isotope system in seawater and carbonates as a paleo-pH proxy. The lack of such knowledge is at least partly responsible for some of the uncertainties in paleo-pH values determined using the boron isotopic composition of marine carbonates and limits the possibility of obtaining absolute values for paleo-pH using the boron isotopic composition of carbonates. It seems clear that mechanisms of boron incorporation cannot be deduced from macroscopic measurements and experiments alone, and that molecular-scale studies are needed to obtain representative information of surface processes occurring during boron coprecipitation with calcite. The aim of this work was to perform in situ Atomic Force Microscopy (AFM) observations and kinetic measurements during calcite growth experiments from B-bearing solutions, under different conditions of pH and supersaturation, in order to improve our understanding of the mechanisms of boron incorporation into carbonates and thereby progressing towards a more accurate use of boron isotopes in carbonates as a paleo-pH proxy.

2. Methodology

In situ observations and measurements of the $\{10\bar{1}4\}$ calcite surfaces during growth were performed using a fluid cell of a Digital Instruments Nanoscope III Multimode AFM working in contact mode under ambient conditions (T=23 °C). AFM images were collected using Si_3N_4 tips (Bruker, probe model NP-S20) with spring constants 0.12 N m^{-1} and 0.58 N m^{-1}. Images were analyzed using the NanoScope software (Version 5.31r1). Freshly cleaved calcite surfaces (Iceland spar, Chihuahua, Mexico), ca. $4\times3\times1$ mm^3 in size, were used as substrates for the AFM experiments. At the start of each growth experiment, doubly-deionised water (resistivity > 18 mΩ cm^{-1}) was passed over the cleaved $\{10\bar{1}4\}$ calcite surfaces to clean the cleaved surface, as well as to adjust the AFM parameters as described in Arvidson et al. (2006). This leads to retreat of pre-existing steps and to the formation of rhombohedral etch pits, defined by steps parallel to the $[\bar{4}41]$ and $[48\bar{1}]$ directions. Thus, the crystallographic orientation of the calcite substrate could be unambiguously established by direct observation of the development of such etch pits before each growth experiment.

Once the directions on the calcite substrate were known, Ca^{2+}–CO_3^{2-}–HBO_3 solutions with the concentrations shown in Table 1 were injected into the fluid cell of the AFM (Set A). In a second set of experiments (Set B), after dissolving the calcite cleaved surface in deionized water, B-free growth solutions were first injected into the fluid cell for enough time to allow development of growth spirals and subsequently, B-bearing solutions were flowed over the surface. We focused our study on these growth hillocks, as information regarding velocity anisotropy of non-equivalent steps on the calcite cleavage plane can be more easily obtained from a detailed study of the growth kinetics of spiral hillocks (Larsen et al., 2010). This protocol allows for the determination of the effect of boron on non-equivalent step kinetics. Spiral hillocks grown around screw dislocations exhibit a polygonized pyramidal geometry and are formed by growth layers each bounded by two obtuse and two acute step edges,

Table 1
Composition of solutions used in AFM growth experiments. Ω_{Cc} is the supersaturation of the solution with respect calcite and $a_{Ca^{2+}}/a_{CO_3^{2-}}$ refers to the ratio of the activities of Ca^{2+} and CO_3^{2-} ions in the growth solutions.

Experiment	Ω_{Cc}	*pH*	$a_{Ca^{2+}}/a_{CO_3^{2-}}$	[*NaHCO$_3$*] (*mM*)	[*CaCl*]$_2$ (*mM*)	[*NaCl*] (*mM*)	[*B*] (*ppm*)
BCC001	6.5	10.0	1.0	0.693	0.419	100	4.5
BCC002	6.5	9.5	1.0	2.071	0.419	98	4.5
BCC003	6.5	9.0	1.0	5.120	0.424	95	4.5
BCC004	6.5	8.5	1.0	14.790	0.440	85	4.5
BCC005	6.5	8.0	1.0	45.850	0.492	55	4.5
BCC006	1.5	10.0	1.0	0.521	0.191	100	4.5
BCC007	1.5	9.5	1.0	0.981	0.191	98	4.5
BCC008	1.5	9.0	1.0	2.442	0.193	95	4.5
BCC009	1.5	8.5	1.0	7.085	0.197	95	4.5
BCC010	1.5	8.0	1.0	21.950	0.208	80	4.5
BCC011	6.5	10.0	1.0	0.698	0.422	100	45
BCC012	6.5	9.5	1.0	2.085	0.422	98	45
BCC013	6.5	9.0	1.0	5.133	0.426	95	45
BCC014	6.5	8.5	1.0	14.810	0.441	85	45
BCC015	6.5	8.0	1.0	45.860	0.493	55	45
BCC016	1.5	10.0	1.0	0.523	0.191	100	45
BCC017	1.5	9.5	1.0	0.983	0.192	98	45
BCC018	1.5	9.0	1.0	2.432	0.191	95	45
BCC019	1.5	8.5	1.0	7.085	0.197	95	45
BCC020	1.5	8.0	1.0	21.950	0.208	80	45

parallel to $[\bar{4}41]_+$, $[48\bar{1}]_+$, $[\bar{4}41]_-$ and $[48\bar{1}]_-$ directions. The subscripts (+ or −) follow the convention used by Paquette and Reeder (1995). The structurally equivalent $[\bar{4}41]_-$ and $[48\bar{1}]_-$ steps are acute and intersect the bottom of the etch pit at an angle of 78°, while $[\bar{4}41]_+$ and $[48\bar{1}]_+$ steps are obtuse and intersect the bottom of the etch pit at an angle of 102° (Hay et al., 2003). Measurements of geometric relationships of the spiral growth hillocks were made from sequential AFM images scanned in the same direction. These measurements enable the determination of the absolute growth velocities of obtuse (v_o) and acute (v_a) steps as described by Larsen et al. (2010). The length x and the angles ϕ and γ, as well as the time lapse, t, between AFM images, can be used to calculate the growth velocities for the obtuse and acute steps using the equations:

$$v_o = \frac{\sin((\phi+\gamma)/2)}{t} \times x$$

$$v_a = \frac{\sin((\phi-\gamma)/2)}{t} \times x$$

where x represents the distance from the pyramid apex to the obtuse/acute corner of the pyramid, γ the angle between two equivalent step edges and ϕ the angle between the two lines joining the pyramid apex to the obtuse/acute corners of the pyramid. Solutions used in the experiments were prepared using double-deionized water (resistivity > 18 mΩ cm^{-1}) and the solution pH was adjusted using HCl or NaOH. Experiments were performed at ionic strength (IS) of 0.1 (adjusted using NaCl). The solution stoichiometry, defined as the ratio of the activities of lattice ions in solution ($a_{Ca^{2+}}/a_{CO_3^{2-}}$), was made equal to ca. 1 by adjusting the amount of $NaHCO_3$ and $CaCl_2$ in the growth solution. The supersaturation, Ω, was calculated by $\Omega = IAP/K_{sp}$ where IAP is the ion activity product and K_{sp} the solubility product of calcite ($10^{-8.48}$, phreeqc.dat database) at 25 °C. Constant composition of the growth solutions was achieved by continuously flowing fresh solutions at ca. 60 mL h^{-1} from a syringe coupled to an O-ring-sealed fluid cell containing the sample crystal. This flow rate is high enough to ensure surface control of the growth rate, in agreement with many of the published AFM experiments that address both calcite dissolution (e.g., Liang et al., 1996) and growth (e.g., Teng et al., 1998).

Attempts were made to quantify boron concentration in the calcite crystals after the flow-through experiments by LA-ICP MS. ^{11}B was detected in the crystal; however, it was not possible to detect ^{10}B as it interferes with Ne^{++} (doubly-charged Neon) and gives a continuous high signal. This prevents boron quantification by the available techniques, but nevertheless the LA-ICP-MS did indicate that boron was incorporated into the crystal.

3. Results

3.1. Experimental Set A—Interactions of boron-bearing solutions and calcite cleavage surfaces

Closure of the dissolution pits was immediately observed upon the injection of growth solutions, and further growth proceeded by the advancement of pre-existing monomolecular (~3 Å) steps (at Ω=1.5). In experiments performed at Ω=6.5, subsequent growth occurs by 2D nucleation and spreading of typical rhombohedral islands, except at pH > 9.0 (B=4.5 ppm) or 9.5 (B=45 ppm), where jagged steps and irregular islands were observed. As well, the formation of numerous defects in the newly grown materials (seen as holes in the AFM images) (Fig. 1) was observed.

Interestingly, at low supersaturation (Ω=1.5), the growing step edges became jagged or dendritic for most of the pH values tested (pH 8–10). Fig. 2 illustrates this type of growth from solutions with [B]=4.5 ppm and 45 ppm. In general, the distance between lobules in the dentrites decreased with increasing boron concentration. Depending on pH, the closure of etch pits can be significantly fast. However, when a new growth layer (L2 in Fig. 3) reached an area that had been already covered by the newly grown material (L1 in Fig. 3), such as the filled-in etch pits, the advancement of steps temporarily stopped. This effect leads to the reproduction of the original calcite microtopography (see in Fig. 3 how etch pits existing in the surface before injecting the growth solution—Fig. 3a—are revealed in subsequent growth layers—Fig. 3c and h). Such an effect has been previously described in a number of calcite and barite growth experiments in the presence of incorporated ions and is commonly known as the *template effect* (Astilleros et al., 2003, 2006; Pérez-Garrido et al., 2009). Further growth proceeded through the formation of irregular lobules or 'fingers' at the step edges, repeating the process. Under these conditions, etch pit did not close uniformly, but was filled from one corner. Another interesting feature observed in the AFM images is that newly grown $[\bar{4}41]_+$ and $[48\bar{1}]_+$ step edges contrasted with the rest of the surface (Fig. 4a). This can be clearly seen in Fig. 4c, which is a detailed height image of the area marked in Fig. 4a. Brighter areas correspond to higher areas in AFM height images. In this image, the newly grown edges appear higher than the initial steps. Measurements along a–a′

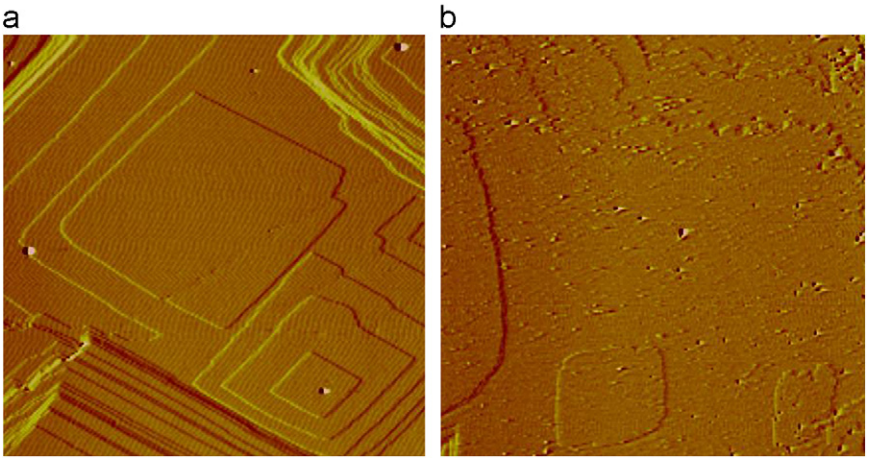

Fig. 1. AFM deflection images of a calcite cleavage surface after the injection of a growth solution (Ω=6.5, [B]=4.5 ppm, $a_{Ca^{2+}}/a_{CO_3^{2-}}=1$) of pH 10 (a) and 9.5 (b). Note the formation of holes or defects during the growth of the new material.

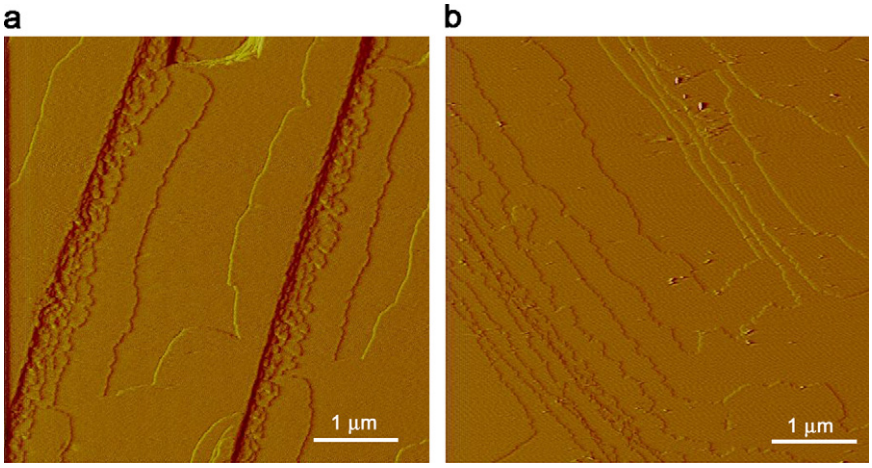

Fig. 2. AFM deflection images of a calcite cleavage surface after the injection of a growth solution ($\Omega=1.5$, pH 10, $a_{Ca^{2+}}/a_{CO_3^{2-}}=1$), with [B]=4.5 ppm (a) and 45 ppm (b). Note the development of jagged or dendritic steps which are not observed in pure (i.e. B-free) growth solutions.

show a difference in height of ca. 1.0 Å between the flat terrace and the edge of the etch pit (Fig. 4b). All the above described features were observed at $\Omega=1.5$ regardless of the pH of the growth solution.

3.2. Experimental Set B—The effect of boron in solution on the kinetics of non-equivalent step advancement

Fig. 5 shows step-spreading rates (v_o and v_a), overall spreading rate (v_{sum}) and v_o/v_a as a function of solution pH, for a constant solution stoichiometry (Ca^{2+} to CO_3^{2-} activity ratio of 1) and driving force. In pure solutions (i.e. B-free), v_a was found to continuously decrease with increasing pH, reaching a plateau when approaching the maximum pH tested in this study (pH 10). On the contrary, both v_o and v_{sum} vs. pH plots show a minimum located ca. pH 8. The ratio v_o/v_a increased continuously with increasing pH, from values of 1.75 up to ca. 14 in pure solutions. This is reflected in a change in the geometry of the growth hillocks, with the angle ϕ decreasing from ca. 150° (pH 8) down to ca. 110° (pH 9.5) (see Fig. 6). Furthermore, it was found that increasing the pH of the growth solutions increased obtuse terrace widths (λ_+), resulting in a decrease in the density of steps on the growth spiral.

The acute step-spreading rate was not significantly modified in the presence of boron for all pH and supersaturation conditions tested in this study, compared to growth from pure solutions under the same conditions. Furthermore, at $\Omega=6.5$ the presence of boron did not result in any significant modification of obtuse step-spreading rates at pH ≤ 9.0. However, at pH > 9.0, v_o was reduced when boron was added to the growth solutions ($\Omega=6.5$). Conversely, at lower supersaturation ($\Omega=1.5$) the effect of boron on obtuse step velocity was evident even at pH 8.5. The parameter v_o/v_a allows direct comparison of the effect of boron on calcite growth kinetics for the different conditions tested in this study. At pH > 9.0, v_o/v_a was significantly reduced when boron was present in solution (Fig. 5d). This indicates that the obtuse step-spreading was retarded relative to acute steps in the presence of boron. Again, the reduction in obtuse step velocity relative to acute step velocity was more evident at $\Omega=1.5$ (Fig. 7). Interestingly, increasing the boron concentration from 4.5 to 45 ppm did not significantly enhance this effect. However, increasing the boron concentration at constant pH and supersaturation caused a decrease in terrace widths at pH > 8.5.

The morphology of the growth spirals remained unaffected by the presence of boron at $\Omega=6.5$ for all pH values tested. Calcite hillocks were characterized by well-formed vicinal faces and straight step-edges. However, changes in hillock morphology were observed in experiments performed closer to equilibrium ($\Omega=1.5$) and at pH 9.5, this being more evident at the highest boron concentration tested. Step edges appeared rougher, and preferentially affected those steps along the positive directions (Fig. 8).

4. Discussion

4.1. Effect of pH on the kinetics of non-equivalent step spreading during calcite growth

Most calcite growth studies so far have been performed at a constant pH of ca. 8 or 10. To our knowledge, just two studies have specifically addressed the effect of pH on calcite growth kinetics, systematically varying the pH of the growth solutions and keeping other solution parameters, such as the degree of supersaturation or the $a_{Ca^{2+}}/a_{CO_3^{2-}}$ activity ratio, constant (Tai et al., 2006; Ruiz-Agudo et al., 2010). The study by Tai et al. (2006) is based on macroscopic measurements of calcite growth rates. Ruiz-Agudo et al. (2010) studied the effect of pH on calcite growth from in situ AFM observations. The general trend of the overall spreading rate (v_{sum}) with pH reported there (with a minimum at pH around 8) is in good agreement with the v_{sum} observed in this study. Nevertheless, in this previous paper growth rates were estimated from measurements of 2D islands, and therefore, differences in pH-sensitivity of non-equivalent step propagation rates were not explored.

The ratio of obtuse to acute step velocity (v_o/v_a) gives information regarding the differential influence of pH on obtuse and acute step spreading rates. If both were affected to the same extent by pH, v_o/v_a would show a constant value independent of the pH of the growth solution. However, v_o/v_a ratios measured in this study indicate that during growth from pure (i.e. B-free) solutions, the rate of obtuse step spreading is progressively accelerated relative to the acute step with increasing pH. This is indirect evidence that the kinetics of obtuse and acute advancement is controlled by different mechanisms at the atomistic level. A similar argument has been used to explain the different sensitivities of obtuse and acute spreading rate to supersaturation, solution stoichiometry or changes in the background electrolytes (Ruiz Agudo et al., 2011).

The observed trend of v_o/v_a as a function of pH can be explained by considering that both Ca^{2+} and $CaCO_3^0$ are incorporated during calcite growth. The relatively strong hydration of the calcium ion represents a kinetic barrier for its incorporation

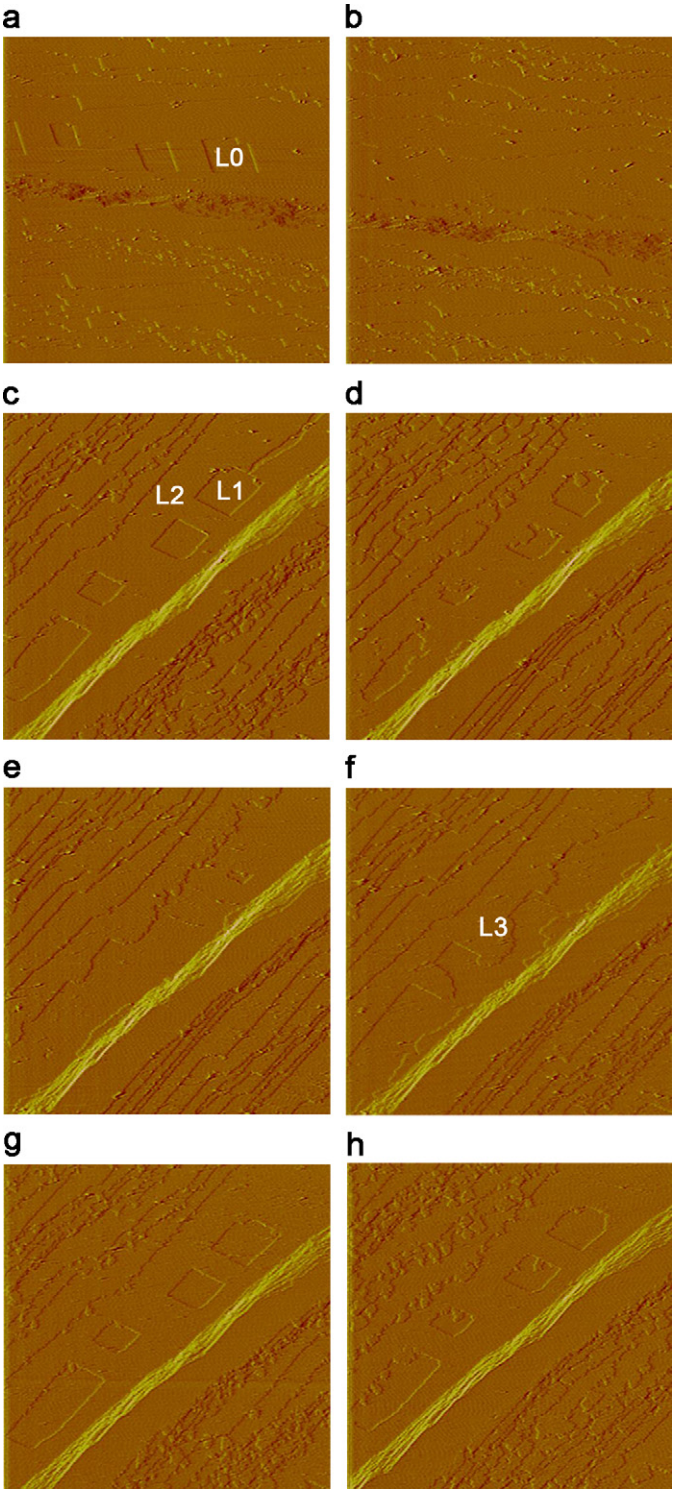

Fig. 3. Sequence of AFM deflection images of a calcite cleavage surface after the injection of (a) pure water and (b–h) a growth solution (Ω=1.5, pH 8, $a_{Ca^{2+}}/a_{CO_3^{2-}}=1$) with [B]=45 ppm. The time lapse between consecutive images is ca. 120 s. When a new growth layer (L2) reached an area that had been already covered by the newly grown material (L1), the advancement of the growth front is temporarily stopped, leading to the reproduction of the original topography (i.e. etch pits) of the surface. (a) and (b) are rotated 45° anticlockwise with respect to the rest of the images.

during growth. However, with increasing pH, the presence of OH^- could effectively increase the frequency of water exchange around Ca^{2+}, thus facilitating its incorporation into calcite (Ruiz Agudo et al., 2011). This effect should, in principle, be reflected equally in both acute and obtuse step advancement. However, as recently suggested (Ruiz Agudo et al., 2011), the rate of dehydration of carbonate surface sites for cation attachment and subsequent kink nucleation controls the velocity of acute step propagation, while dehydration of calcium ions in solution appears to determine the rate of obtuse step spreading. This would explain why obtuse step spreading is accelerated relative to acute step upon increasing pH and consequently calcium ion dehydration in solution.

4.2. Interaction of boron species with calcite during growth: Incorporation into non-structural sites

The results of this AFM study show a strong interaction of boron species with calcite {10$\bar{1}$4} surfaces during growth, this being most evident at low supersaturation (Ω=1.5) and high pH ($\geq$9.0). In particular, the observation that the advancement of growth steps is blocked at buried step edges reproducing the topography of the original substrate suggests a dimensional or height difference between the newly grown material and the underlying substrate (*template effect*, Astilleros et al., 2003). This is likely to be caused by changes in lattice parameters due to the incorporation of boron into the calcite structure, either in structural sites or defect positions.

Hemming et al. (1995) reported a significant increase in the partition coefficient for boron into calcite with decreasing boron concentration in the fluid below 5 ppm, while the partition coefficient remained constant for concentrations greater than ca. 5 ppm. This observation is in agreement with the small differences detected in our experiments when B concentration was increased from 4.5 to 45 ppm. Hemming et al. (1995) explained this effect assuming a multiple-site incorporation mechanism in which boron is incorporated into calcite substituting for carbonate in lattice sites as well as in a limited number of non-lattice (defect) sites, which become saturated at low boron concentration (ca. 5 ppm). An equivalent mechanism has been proposed to explain the dependence of the partition coefficient of Sr^{2+} into calcite on Sr^{2+} concentration in solution (Pingitore and Eastman, 1986). Such a mechanism is consistent with the observations reported here regarding the anomalous thickness of step edges growing in continuity with pre-existing steps in the original calcite substrate (see above). When B-doped calcite grows in continuity with pre-existing steps (Set A), the thick step edges detected in some of the experiments suggest that at least part of the boron may be incorporated into non-lattice (defect) sites in calcite. Incorporation of foreign ions in non-lattice calcite sites may result in an anomalous deformation of the {10$\bar{1}$4} planes, which is reflected in the higher step thickness (Astilleros et al., 2000).

4.3. Effect of boron on the kinetics of non-equivalent calcite step advancement

The presence of boron results in a decrease in the obtuse step rate relative to the acute step rate, only noticeable at pH > 9 for Ω=6.5 and at pH > 8 for Ω=1.5. This indicates that boron retards the spreading of obtuse steps at the highest pH values tested compared to growth from pure solutions at the same pH, supersaturation and solution stoichiometry. The stronger effect observed at high pH is in agreement with the basic assumption of tetrahedrally-coordinated boron being mainly incorporated into calcite, which is the dominant boron aqueous species at pH > 9.25. However, early MAS NMR spectroscopy analysis of boron coordination in carbonates showed that boron is predominantly trigonally coordinated in calcite (90%) (Sen et al., 1994). To reconcile these observations, it is assumed that a change in the

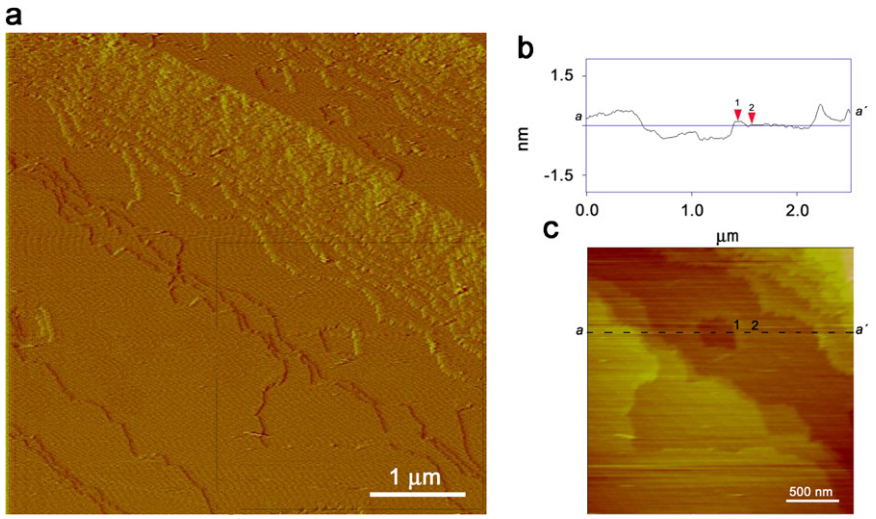

Fig. 4. (a) AFM deflection image showing a calcite cleavage surface after the injection of a growth solution (Ω=1.5, pH 9.5, $a_{Ca^{2+}}/a_{CO_3^{2-}}=1$) with [B]=45 ppm. Note how the newly grown step edges contrast with the rest of the surface. (b) Depth profile in section aa′ (c) detailed topographic image of the area shown in (a).

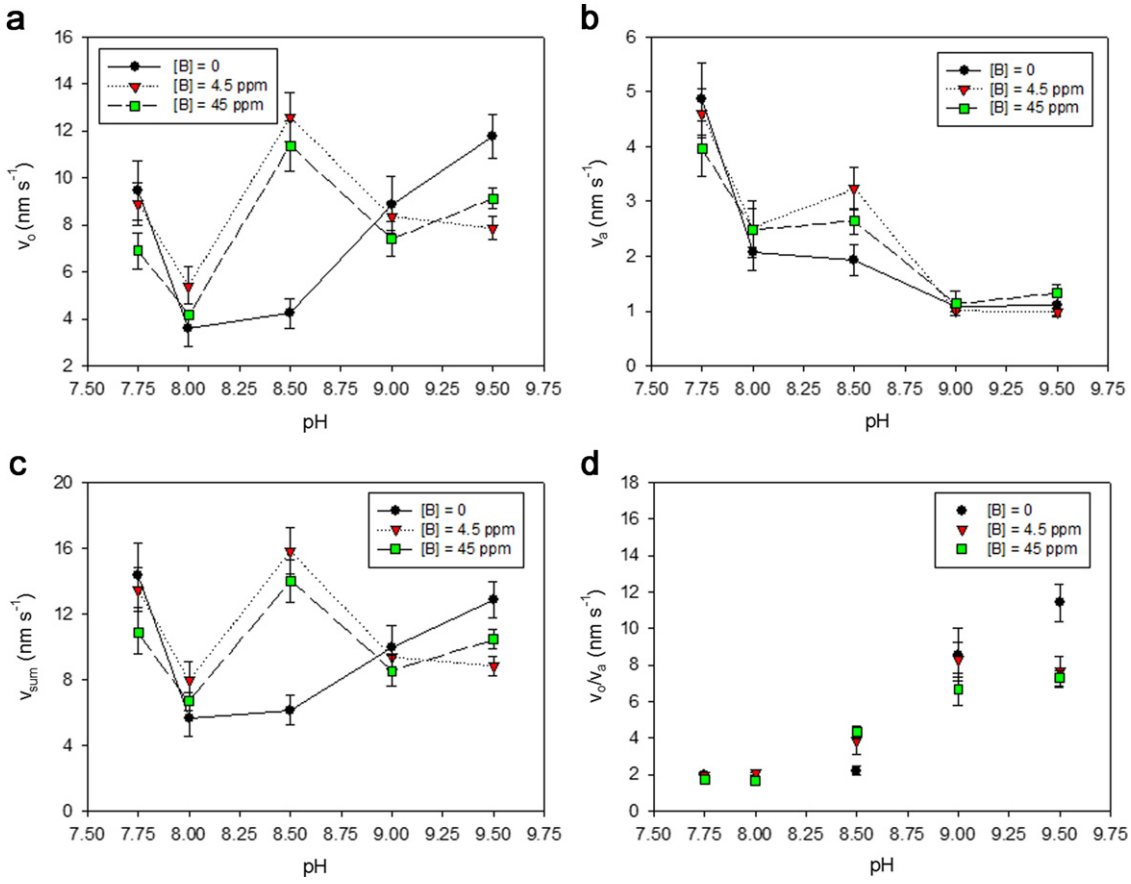

Fig. 5. (a) Obtuse (v_o) and (b) acute (v_a) step propagation velocities, (c) overall spreading rate (v_{sum}) and (d) v_o/v_a as a function of solution pH and boron concentration for a constant solution stoichiometry ($a_{Ca^{2+}}/a_{CO_3^{2-}}=1$) and driving force ($\Omega$=1.5).

first-shell coordination of boron should occur, from tetrahedral in solution to trigonal in calcite (Sen et al., 1994; Hemming et al., 1998; Klochko et al., 2009). Nevertheless, this aspect remains controversial, as it has been shown recently by Klochko et al. (2009) that trigonally and tetrahedrally coordinated boron are almost equally present in biogenic and inorganic carbonates. The larger positive deviations of δ^{11}B in carbonates relative to aqueous borate found at lower pH is the argument used by these authors to suggest that the incorporation of trigonally-coordinated boron is important at lower pH, as could be expected due to the fact that the relative concentration of trigonally-coordinated boron increases with decreasing pH. If boric acid was actually incorporated into carbonates together with borate, the overall boron isotopic composition would be higher than expected if only borate was incorporated, as boric acid is enriched in ^{11}B relative to the tetrahedral species. However, the significant presence of boron in trigonal coordination shown by Klochko et al. (2009) would imply a much higher enrichment in ^{11}B than

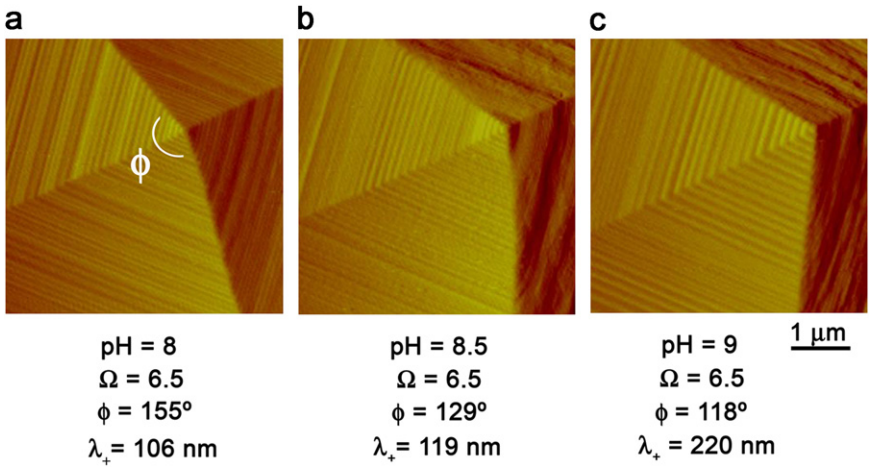

Fig. 6. AFM deflection images of hillocks grown around screw dislocations in pure (i.e. B-free) supersaturated solutions of $a_{Ca^{2+}}/a_{CO_3^{2-}}=1$ and $\Omega=6.5$ and different pHs: (a) pH=8, (b) pH=8.5 and (c) pH=9.

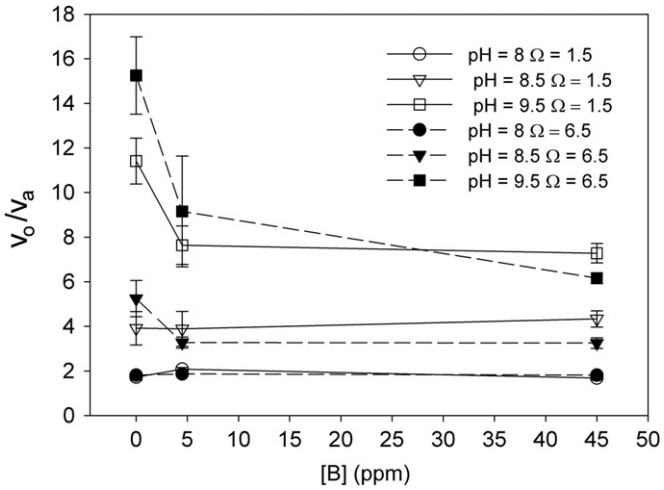

Fig. 7. v_o/v_a as a function of solution pH, boron concentration and supersaturation for a constant solution stoichiometry ($a_{Ca^{2+}}/a_{CO_3^{2-}}=1$).

that reported in the literature for both biogenic and inorganic carbonates. Therefore, it seems that a change in coordination from trigonal to tetrahedral does certainly occur. Our AFM observations show no effect of boron on calcite growth at low pH values (at $\Omega=6.5$), thus suggesting that the extent of boron incorporation under these conditions could be limited. Furthermore, we suggest the possibility that the coordination change from tetrahedral to trigonal may be the limiting factor for boron incorporation into calcite. This could be another explanation for the fact that only small differences were observed in our experiments when the B concentration was increased from 4.5 to 45 ppm, and also that the measured boron partition coefficient remained constant for fluid boron concentrations greater than ca. 5 ppm (Hemming et al., 1995). This argument has been also used to explain why boron is preferentially incorporated into aragonite relative to calcite, as such a change in boron coordination is necessary for its incorporation into calcite, but not into aragonite, which is consistent with the different boron coordination determined in the two polymorphs (Hemming et al., 1995). Furthermore, it leads us to hypothesize that differences in calcite growth rates may result in variations in the relative proportions of trigonally and tetrahedrally coordinated boron found in carbonate samples (Sen et al., 1994; Klochko et al., 2009; Rollion-Bard et al., 2011), associated with the time needed for the change in coordination to occur and not with the fact that both species were actually incorporated. Also, the fact that our results suggest that tetrahedrally-coordinated boron is the main species incorporated into calcite implies that there should be some isotopic fractionation associated with the change in coordination from tetrahedrally-coordinated to trigonally-coordinated boron that would explain the offset found between $\delta^{11}B$ in carbonates and the solution from which they precipitated. The study of this fractionation process is beyond the scope of this paper but certainly deserves further investigation.

At high pH, when tetrahedrally-coordinated boron is the main species in solution, and thus can be effectively incorporated into calcite, strong effects on calcite growth were observed, as reflected in the rounding and roughening of steps, as well as in the reduction of the relative rate of obtuse step spreading. These observations are in agreement with those by Hemming et al. (1995) who reported the strong curvature and rounding of steps resulting in changes in the morphology of growth hillocks in crystals precipitated from solutions containing 500 ppm boron. Furthermore, our findings suggest that $B(OH)_4^-$ selectively interacts with calcite growth steps and give indirect evidence for the preferential incorporation of $B(OH)_4^-$ at obtuse steps. From a structural point of view, it seems reasonable to suggest that $B(OH)_4^-$ species will fit better in a less constrained space, as they are much larger than trigonal boron and carbonate ions. B-selective incorporation into calcite has been previously reported by Hemming et al. (1998). However, our observations contradict the result reported by these authors, who detected higher boron concentrations in acute steps relative to obtuse steps in their ion microprobe analysis of B-doped calcite single crystals.

It is however difficult to compare the present set of experiments with those resulting in the precipitation of the crystals analyzed by Hemming and co-workers, as they were performed under totally different conditions (Hemming et al., 1995). In particular, their experiments were carried out exclusively at pH ca. 8. As stated above, no significant evidence of interaction (neither in obtuse nor in acute steps) between boron and calcite surfaces was observed under these conditions in our AFM experiments, thus making it impossible to extract any information regarding the preferential incorporation of boron at any specific step on a calcite surface at pH 8. However, in agreement with our observations, Hemming et al. (1995) concluded that in their experiments only tetrahedrally-coordinated boron interacts with the calcite surface. This conclusion is based on the fact that the isotopic composition of the precipitated calcite is identical to the boron isotopic composition of tetrahedrally-coordinated boron in

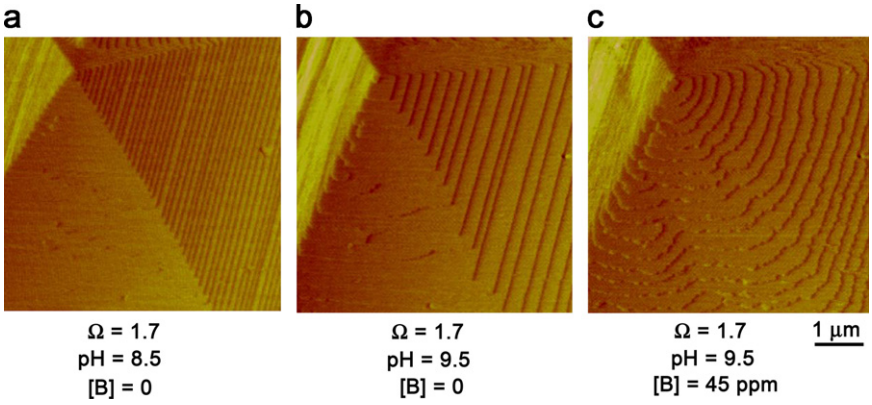

Fig. 8. AFM deflection images of hillocks grown around screw dislocations in supersaturated solutions of $a_{Ca^{2+}}/a_{CO_3^{2-}}=1$ and $\Omega=1.5$: (a) pH=8.5, [B]=0; (b) pH=9.5, [B]=0 and (c) pH=9.5, [B]=45 ppm. Note the development of jagged steps in the presence of boron.

the growth solutions, calculated using a fractionation factor similar to that proposed by Kakihana et al. (1977).

We hypothesize that the preferential incorporation in obtuse steps observed in our experiments is not linked to the fact that boron species are incompatible with calcite ($K_d<1$) and thus should be incorporated in the faster growing steps. In fact, the stronger effects of boron on calcite growth are observed at $\Omega=1.5$, although under these conditions the velocity of both acute and obtuse step spreading is lower than at $\Omega=6.5$. Enhanced effects of boron on calcite growth at lower supersaturation may be associated with the above-mentioned change from tetrahedrally-coordinated to trigonally-coordinated boron upon adsorption into calcite surfaces. At slow growth rates, once tetrahedrally-coordinated boron is adsorbed onto the carbonate surface, there would be sufficient time for such a change in coordination to occur just prior to incorporation; this may result in increased stability of tetrahedrally-coordinated boron relative to carbonate, therefore increasing its partitioning into calcite. These results differ from those by Hobbs and Reardon (1999), who reported higher boron incorporation in calcite crystals precipitated from vaterite-saturated solutions compared to crystals grown from aragonite-saturated solutions (with a lower saturation state with respect to calcite and thus a lower growth rate). However, in their experiments, pH varied together with Ca/CO_3 activity ratio, which has been shown to significantly alter calcite growth kinetics (Nehrke et al., 2007; Perdikouri et al., 2009; Stack and Grantham 2010; Larsen et al., 2010). Furthermore, in the case of calcite precipitation from aragonite-saturated solutions, most of the crystals showed non-rhombohedral crystallographic forms and thus the differential incorporation of boron onto specific calcite faces may also play a role in the different effect of the growth rate observed by Hobbs and Reardon (1999) and inferred in the present study. Development of crystallographic forms different from the equilibrium, rhombohedral form has also been recently reported in calcite crystals grown from pure solutions at alkaline pH (Ruiz-Agudo et al., 2010).

5. Conclusions and implications

Our in situ AFM observations show significant interactions of boron and calcite surfaces during growth, particularly at high pH (>9.0) and low solution supersaturation. These interactions are step-specific, as shown by the rounding and roughening of obtuse steps as well as the reduction in the obtuse step-spreading rate, and are stronger at high pH (9.5) and close to equilibrium. Overall, the results of this study indicate that changes in growth rate are a key factor (together with the pH of the calcifying fluid) to consider when using boron in biocarbonates as a pH proxy, as these factors could influence the amount of boron incorporated and, possibly, its isotopic signature. In comparison with other inorganic studies of coprecipitation, we suggest that the calcite crystallographic form in which boron is incorporated is also a critical factor controlling the amount of boron incorporated.

Therefore, given the results of this study, care must be taken when interpreting trends in the boron composition of marine carbonates. In principle, a decrease in oceanic pH as a consequence of increased atmospheric CO_2 concentrations would lead to a decrease in the saturation state of the calcifying fluids, resulting in slower calcification rates, which, according to our observations, would enhance boron incorporation. On the contrary, this decrease in pH would also result in a decrease in the relative concentration of tetrahedrally-coordinated boron which according to our results seems to be the main active boron species in seawater relevant to incorporation into carbonates, this therefore leading to a decrease in boron incorporation. The balance between these two opposite effects will determine the final influence of pH on the amount of boron incorporation. Furthermore, the fact that tetrahedrally-coordinated boron is the main species incorporated into calcite leads us to hypothesize that isotopic fractionation should occur to some extent during the change in coordination from tetrahedral (in solution) to trigonal (in calcite) and that may explain the offset reported between $\delta^{11}B$ in carbonates and the solution from which they precipitated. Thus the relationship between boron composition and seawater pH cannot be as straightforward as suggested by previous proposed correlations. Aside from problems associated with the lack of knowledge of the chemistry of the calcifying fluid, we suggest that kinetic effects related to changes in growth rate may also help to explain some of the variability of the data reported in the literature. Therefore, developing growth rate corrections for boron content in marine biocarbonates seems critical for its accurate use as a pH proxy. In our opinion, progress towards this objective requires new controlled culture experiments focused on species with different calcification rates that also include textural studies and micro-sensor analyses of calcifying fluids.

Acknowledgments

This work was performed within the EU Initial Training Network Delta-Min (Mechanisms of Mineral Replacement Reactions) Grant PITN-GA-2008-215360 at the University of Münster, Germany. E. Ruiz-Agudo also acknowledges the University of Granada (Spain) for subsequent financial support through a reintegration Grant (Plan Propio Program) and the Spanish

Ministry of Science and Education for a Ramón y Cajal Grant. Experimental facilities in Munster are supported by the Deutsche Forschungsgemeinschaft (DFG). Additional funding was provided by the research group RNM-179 (Junta de Andaluci´a, Spain). We are thankful to three anonymous reviewers for the constructive comments that have helped us to improve the overall quality of this manuscript.

References

Al-Horani, F.A., Al-Moghrabi, S.M., de Beer, D., 2003. The mechanism of calcification and its relation to photosynthesis and respiration in the scleractinian coral *Galaxea fascicularis*. Mar. Biol. 142, 419–426.

Arvidson, R.S., Collier, M., Davis, K.J., Vinson, M.D., Amonette, J.E., Luttge, A., 2006. Magnesium inhibition of calcite dissolution kinetics. Geochim. Cosmochim. Acta 70, 583–594.

Astilleros, J.M., Pina, C.M., Fernández-Díaz, L., Putnis, A., 2003. Nanoscale growth of solids crystallising from multicomponent aqueous solutions. Surf. Sci. 545, L767–L773.

Astilleros, J.M., Pina, C.M., Fernández-Díaz, L., Putnis, A., 2000. The effect of barium on calcite (10–14) surfaces during growth. Geochim. Cosmochim. Acta 64, 2965–2972.

Astilleros, J.M., Pina, C.M., Fernández-Díaz, L., Prieto, M., Putnis, A., 2006. Nanoscale phenomena during the growth of solid solutions on calcite {10–14} surfaces. Chem. Geol. 225, 322–325.

Dickson, A.G., 1990. Thermodynamics of the dissociation of boric acid in synthetic seawater from 273.15 to 318.15 K. Deep-Sea Res. 37, 755–766.

Gaillardet, J., Allègre, C.J., 1995. Boron isotopic compositions of corals: seawater or diagenesis record? Earth Planet. Sci. Lett. 136, 665–676.

Hay, M.B., Workman, R.K., Manne, S., 2003. Mechanisms of metal ion sorption on calcite: composition mapping by lateral force microscopy. Langmuir 19, 3727–3740.

Hemming, N.G., Hanson, G.N., 1992. Boron isotopic composition and concentration in modern marine carbonates. Geochim. Cosmochim. Acta 56, 537–543.

Hemming, N.G., Reeder, R.J., Hanson, G.N., 1995. Mineral–fluid partitioning and isotopic fractionation of boron in synthetic calcium carbonate. Geochim. Cosmochim. Acta 59, 371–379.

Hemming, N.G., Reeder, R.J., Hart, S.R., 1998. Growth-step-selective incorporation of boron on calcite surface. Geochim. Cosmochim. Acta 62, 2915–2922.

Hobbs, M.Y., Reardon, E.J., 1999. Effect of pH on boron coprecipitation by calcite: further evidence for nonequilibrium partitioning of trace elements. Geochim. Cosmochim. Acta 63, 1013–1021.

Hönisch, B., Hemming, N.G., Loose, B., 2007. Comment on "A critical evaluation of the boron isotope-pH proxy: The accuracy of ancient ocean pH estimates" by M. Pagani, D. Lemarchand, A. Spivack and J. Gaillardet. Geochim. Cosmochim. Acta 71, 1636–1641.

Jorgensen, B.B., Erez, J., Revsbech, N.P., Cohen, Y., 1985. Symbiotic photosynthesis in a planktonic foraminifera *Globigerinoides sacculifer* (Brady), studied with microelectrodes. Limnol. Oceanogr. 30, 1253–1267.

Kakihana, H., Kotaka, M., Satoh, S., Nomura, M., Okamoto, M., 1977. Fundamental studies on the ion-exchange separation of boron isotopes. Bull. Chem. Soc. Jpn. 50, 158–163.

Klochko, K., Kaufman, A.J., Yao, W., Byrne, R.H., Tossell, J.A., 2006. Experimental measurement of boron isotope fractionation in seawater. Earth Planet. Sci. Lett. 248, 261–270.

Klochko, K., Cody, G.D., Tossell, J.A., Dera, P., Kaufman, A.J., 2009. Re-evaluating boron speciation in biogenic calcite and aragonite using ^{11}B MAS NMR. Geochim. Cosmochim. Acta 73, 1890–1900.

Larsen, K., Bechgaard, K., Stipp, S.L.S., 2010. The effect of the Ca^{2+} to CO_3^{2-} activity ratio on spiral growth at the calcite {10$\bar{1}$4} surface. Geochim. Cosmochim. Acta 74, 2099–2109.

Liang, Y., Baer, D.R., McCoy, J.M., Amonette, J.E., LaFemina, J.P., 1996. Dissolution kinetics at the calcite–water interface. Geochim. Cosmochim. Acta 60, 4883–4887.

Nehrke, G., Reichart, G.J., Van Cappellen, P., Meile, C., Bijma, J., 2007. Dependence of calcite growth rate and Sr partitioning on solution stoichiometry: non-Kossel crystal growth. Geochim. Cosmochim. Acta 71, 2240–2249.

Pagani, M., Lemarchand, D., Spivack, S., Gaillardet, J., 2005. A critical evaluation of the boron isotope-pH proxy: the accuracy of ancient ocean pH estimates. Geochim. Cosmochim. Acta 69, 953–961.

Pagani, M., Spivack, S., 2007. Response to the Comment by B. Hönisch, N.G. Hemming, B. Loose on "A critical evaluation of the boron isotope-pH proxy: The accuracy of ancient ocean pH estimates". Geochim. Cosmochim. Acta 71, 1642.

Paquette, J., Reeder, R.J., 1995. Relationship between surface structure, growth mechanism, and trace element incorporation in calcite. Geochim. Cosmochim. Acta 59, 735–749.

Perdikouri, C., Putnis, C.V., Kasioptas, A., Putnis, A., 2009. An atomic force microscopy study of the growth of a calcite surface as a function of calcium/total carbonate concentration ratio in solution at constant supersaturation. Cryst. Growth Des. 9, 4344–4350.

Pérez-Garrido, C., Astilleros, J.M., Fernández-Díaz, L., Prieto, M., 2009. In situ AFM study of the interaction between calcite {10–14} surfaces and supersaturated Mn^{2+}–CO_3^{2-} aqueous solutions. Chem. Geol. 311, 4730–4739.

Pingitore Jr., N.E., Eastman, M.P., 1986. The coprecipitation of Sr^{2+} with calcite at 25 °C and 1 atm. Geochim. Cosmochim. Acta 50, 2195–2203.

Rollion-Bard, C., Erez, J., 2010. Intra-shell boron isotope ratios in the symbiont-bearing benthic foraminiferan *Amphistegina lobifera*: implications for δ^{11}B vital effects and paleo-pH reconstructions. Geochim. Cosmochim. Acta 74, 1530–1536.

Rollion-Bard, C., Blamart, D., Trebosc, J., Tricot, G., Mussi, A., Cuif, J.-P., 2011. Boron isotopes as pH proxy: a new look at boron speciation in deep-sea corals using ^{11}B MAS NMR and EELS. Geochim. Cosmochim. Acta 75, 1003–1012.

Royal Society, 2005. Ocean Acidification due to Increasing Atmospheric Carbon Dioxide. The Royal Society, London (pp. 57).

Ruiz Agudo, E., Putnis, C.V., Rodriguez-Navarro, C., Putnis, A., 2011. Effect of pH on calcite growth at constant Ca/CO_3 and supersaturation. Geochim. Cosmochim. Acta 75, 284–296.

Ruiz-Agudo, E., Kowacz, M., Putnis, C.V., Putnis, A., 2010. The role of background electrolytes on the kinetics and mechanism of calcite dissolution. Geochim. Cosmochim. Acta 74, 1256–1267.

Sanyal, A., Hemming, N.G., Broecker, W.S., 1997. Changes in pH in the eastern equatorial Pacific across stage 5–6 boundary based on boron isotopes in foraminifera. Global Biogeochem. Cycles 11, 125–133.

Sanyal, A., Hemming, N.G., Hanson, G.N., Broecker, W.S., 1995. The pH of the glacial ocean as reconstructed from boron isotope measurements on foraminifera. Nature 373, 234–236.

Sanyal, A., Nugent, M., Reeder, R.J., Bijma, J., 2000. Seawater pH control on the boron isotopic composition of calcite: evidence from inorganic calcite precipitation experiments. Geochim. Cosmochim. Acta 64, 1551–1555.

Sen, S., Stebbins, J.F., Hemming, N.G., Ghosh, B., 1994. Coordination environments of boron impurities in calcite and aragonite polymorphs: an ^{11}B MAS NMR study. Am. Mineral. 79, 818–825.

Spivack, A.J., You, C.F., Smith, H.J., 1993. Foraminiferal boron isotope ratios as a proxy for surface ocean pH over the past 21 Myr. Nature 363, 149–151.

Stack, A.G., Grantham, M.C., 2010. Growth rate of calcite steps as a function of aqueous calcium-to-carbonate ratio: independent attachment and detachment of calcium and carbonate ions. Cryst. Growth Des. 10, 1409–1413.

Tai, C.Y., Chang, M.-C., Wu, C.-K., Linet, Y.-C., 2006. Interpretation of calcite growth data using the two-step crystal growth model. Chem. Eng. Sci. 61, 5346–5354.

Teng, H.H., Dove, P.M., Orme, C., De Yoreo, J.J., 1998. Thermodynamics of calcite growth: baseline for understanding biomineral formation. Science 282, 724–727.

Trotter, J., Montagna, P., McCulloch, M., Silenzi, S., Reynaud, S., Mortimer, G., Martini, S., Ferrier-Pagès, C., Gattuso, J.-P., Rodolfo-Metalpa, R., 2011. Quantifying the pH 'vital effect' in the temperate zooxanthellate coral *Cladocora caespitosa*: validation of the boron seawater pH proxy. Earth Planet. Sci. Lett. 303, 163–173.

Vengosh, A., Kolodny, Y., Starinsky, A., Chivas, A.R., McCulloch, M.T., 1991. Coprecipitation and isotopic fractionation of boron in modern biogenic carbonates. Geochim. Cosmochim. Acta 55, 2901–2910.